AGU PUBLICATIONS

JGR

Journal of Geophysical Research: Biogeosciences

RESEARCH ARTICLE
10.1002/2015JG003240

Key Points:
- Upwelling driven by winds and coastal inflows structure the spring bloom
- Large spatial gradients in biogeochemistry driven by hydrography in the fjord
- Physical and biogeochemical observations close to tidewater glaciers during spring

Correspondence to:
L. Meire,
lorenz.meire@ugent.be

Citation:
Meire, L., J. Mortensen, S. Rysgaard, J. Bendtsen, W. Boone, P. Meire, and F. J. R. Meysman (2016), Spring bloom dynamics in a subarctic fjord influenced by tidewater outlet glaciers (Godthåbsfjord, SW Greenland), *J. Geophys. Res. Biogeosci.*, *121*, 1581–1592, doi:10.1002/2015JG003240.

Received 13 OCT 2015
Accepted 12 MAY 2016
Accepted article online 14 MAY 2016
Published online 18 JUN 2016

Spring bloom dynamics in a subarctic fjord influenced by tidewater outlet glaciers (Godthåbsfjord, SW Greenland)

Lorenz Meire[1,2,3], John Mortensen[2], Søren Rysgaard[2,4,5,6], Jørgen Bendtsen[6,7], Wieter Boone[4], Patrick Meire[8], and Filip J. R. Meysman[3,9]

[1]Marine Biology Laboratory, Ghent University, Ghent, Belgium, [2]Greenland Climate Research Centre, Greenland Institute of Natural Resources, Nuuk, Greenland, [3]Department of Ecosystem Studies, Royal Netherlands Institute of Sea Research (NIOZ), Yerseke, Netherlands, [4]Centre for Earth Observation Science, Department of environment and Geography, University of Manitoba, Winnipeg, Manitoba, Canada, [5]Department of Geological Sciences, University of Manitoba, Winnipeg, Manitoba, Canada, [6]Arctic Research Centre, Aarhus University, Aarhus, Denmark, [7]ClimateLab, Symbion Science Park, Copenhagen, Denmark, [8]Ecosystem Management Research Group, Department of Biology, University of Antwerp, Antwerp, Belgium, [9]Department of Analytical, Environmental and Geochemistry, Vrije Universiteit Brussel, Brussels, Belgium

Abstract In high-latitude fjord ecosystems, the spring bloom accounts for a major part of the annual primary production and thus provides a crucial energy supply to the marine food web. However, the environmental factors that control the timing and intensity of these spring blooms remain uncertain. In 2013, we studied the spring bloom dynamics in Godthåbsfjord, a large fjord system adjacent to the Greenland Ice Sheet. Our surveys revealed that the spring bloom did not initiate in the inner stratified part of the fjord system but only started farther away from tidewater outlet glaciers. A combination of out-fjord winds and coastal inflows drove an upwelling in the inner part of the fjord during spring (April–May), which supplied nutrient-rich water to the surface layer. This surface water was subsequently transported out-fjord, and due to this circulation regime, the biomass accumulation of phytoplankton was displaced away from the glaciers. In late May, the upwelling weakened and the dominant wind direction changed, thus reversing the direction of the surface water transport. Warmer water was now transported toward the inner fjord, and a bloom was observed close to the glacier terminus. Overall, our findings imply that the timing, intensity, and location of the spring blooms in Godthåbsfjord are controlled by a combination of upwelling strength and wind forcing. Together with sea ice cover, the hydrodynamic regime hence plays a crucial role in structuring food web dynamics of the fjord ecosystem.

1. Introduction

Productivity in high-latitude fjords shows a strong seasonal cycle where the start of the productive season is marked by an intense phytoplankton spring bloom [*Sakshaug*, 2004; *Hodal et al.*, 2012]. This spring bloom is responsible for a large part of the annual primary production [*Sakshaug*, 2004] and thus plays an essential role in sustaining the secondary production of these high-latitude fjords. Favorable conditions for spring bloom development typically occur during late March to late April, and physical factors are recognized to play a crucial role in the timing and development of the spring bloom. In the conventional model of spring bloom development, three important factors are controlling the initiation of the spring bloom in high-latitude fjords: sufficient incoming irradiation, the onset of stratification, and the breakup of sea ice [*Eilertsen et al.*, 1989; *Eilertsen and Frantzen*, 2007; *Degerlund and Eilertsen*, 2010; *Hodal et al.*, 2012]. In ice-free regions, high levels of turbulent mixing combined with strong light limitation prevent phytoplankton growth during winter [*Eilertsen and Frantzen*, 2007]. During spring, a rapid increase in irradiance, combined with high nutrient concentrations in the surface waters and the development of a stratified water column, triggers an intense phytoplankton bloom [*Sakshaug*, 2004]. The occurrence of stratification in the surface water is crucial, as stratification limits the transport of cells out of the euphotic zone; the spring bloom develops when the mixed layer shoals to a depth above the critical depth [*Sverdrup*, 1953]. This increased stratification in spring can be temperature driven, i.e. by increasing insolation and elevated air-sea heat exchange, and/or salinity driven, i.e. by sea ice melt or by runoff driven by snow melt or precipitation. Because salinity-driven stratification typically develops first in the inner fjord, where terrestrial runoff enters, it has been hypothesized that the spring bloom characteristically develops earlier in the inner part of fjords [*Tett and Wallis*, 1978; *Syvitski et al.*, 1987].

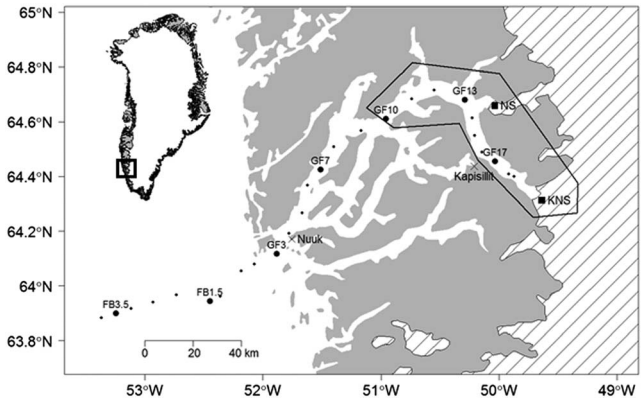

Figure 1. Map of the Godthåbsfjord system and adjacent continental shelf. The indicated area delineates the fjord branch Kangersuneq, which is our main study area. Small solid dots represent the CTD stations visited during the May 2013 cruise. The three monthly monitoring stations (GF10, GF13, and GF17) are indicated in addition to the two main tidewater glaciers (KNS, Kangiata Nunaata Sermia, and NS, Narsap Sermia; bold squares) and the meteorological station (Kapisillit; cross). The white shaded area is the Greenland Ice Sheet.

Presence of (snow-covered) sea ice can, however, strongly impact the timing of the blooms [*Rysgaard and Glud*, 2007], as it limits the penetration of solar radiation into the surface water thus reducing productivity [*Arrigo et al*., 2008]. Sea ice cover can hence postpone the initiation of the spring bloom compared to fjord systems that remain ice free [*Rysgaard and Glud*, 2007]. The breakup of sea ice is therefore often associated with the development of a strong spring bloom as the nutrient-rich water layers are suddenly exposed to increased irradiance. At the same time, sea ice melt also increases water column stability, thus additionally reinforcing the favorable conditions for bloom development [*Rysgaard et al*., 1999; *Wu et al*., 2007]. Here, however, we hypothesize that—in addition to light climate and stratification—there could be another important physical factor controlling the spring bloom dynamics in Arctic fjords. The idea is that the hydrodynamic regime and water circulation pattern within the fjord may modulate the extent and timing of the spring bloom, but up to present, this effect has not been studied in great detail. A recent study in Kongfjorden (Svalbard) observed a clear relation between the spring bloom and coastal inflows and suggested that variations in the timing and magnitude of the coastal inflows could have major implications on timing and extent of the spring bloom [*Hegseth and Tverberg*, 2013].

To investigate the impact of fjord circulation on the spring bloom dynamics in Arctic fjords, we conducted a field study in Godthåbsfjord, located in southwest Greenland. Godthåbsfjord is one of the largest fjord systems in the world and is of great importance for the local fisheries [*Storr-Paulsen et al*., 2004]. The spring bloom plays an important role in the productivity of the fjord and accounts for 50–60% of the total annual primary production [*Juul-Pedersen et al*., 2015; *Meire et al*., 2015]. Previous oceanographic studies in Godthåbsfjord have identified a complex circulation pattern in the fjord system, characterized by coastal inflows during winter and spring [*Mortensen et al*., 2011, 2014]. In 2013, Godthåbsfjord was characterized by an early breakup of the sea ice, and we took advantage of this opportunity to survey the biogeochemistry within the inner parts of the fjord close the tidewater glaciers. The main objective of this study was to investigate whether the hydrodynamic circulation has any effect on the spring bloom in Godthåbsfjord.

2. Material and Methods

2.1. Study Site

Godthåbsfjord is a large fjord system located at 64°N on the southwest coast of Greenland with a length of ~190 km covering a total area of ~2013 km^2 (Figure 1) influenced by three tidewater outlet glaciers located in the innermost part of the fjord [*Mortensen et al*., 2011, 2013]. The fjord system has a complex geometry with several fjord branches and contains several sills, with the main sill (170 m deep) located at the entrance to the fjord. The study area here includes the northernmost fjord branch, Nuup Kangerlua, and the inner part of the fjord, referred to as Kangersuneq (Figure 1). This inner section of the fjord is in direct contact with three tidewater outlet glaciers from the Greenland Ice Sheet: Kangiata Nunaata Sermia (KNS), Akullersuup Sermia (AS), and Narsap Sermia (NS) (Figure 1). During winter, the innermost part of the fjord is typically covered by sea ice, where the ice edge usually extends to station GF13. After the sea ice breakup in late spring, the inner fjord is mostly packed with newly calved glacial ice, and this makes hydrographic sampling near the tidewater outlet glaciers difficult in spring. However, in 2013, sea ice broke up early in the inner part of the fjord, which made sampling possible from March until mid-June in Kangersuneq. On 10 June, the ice

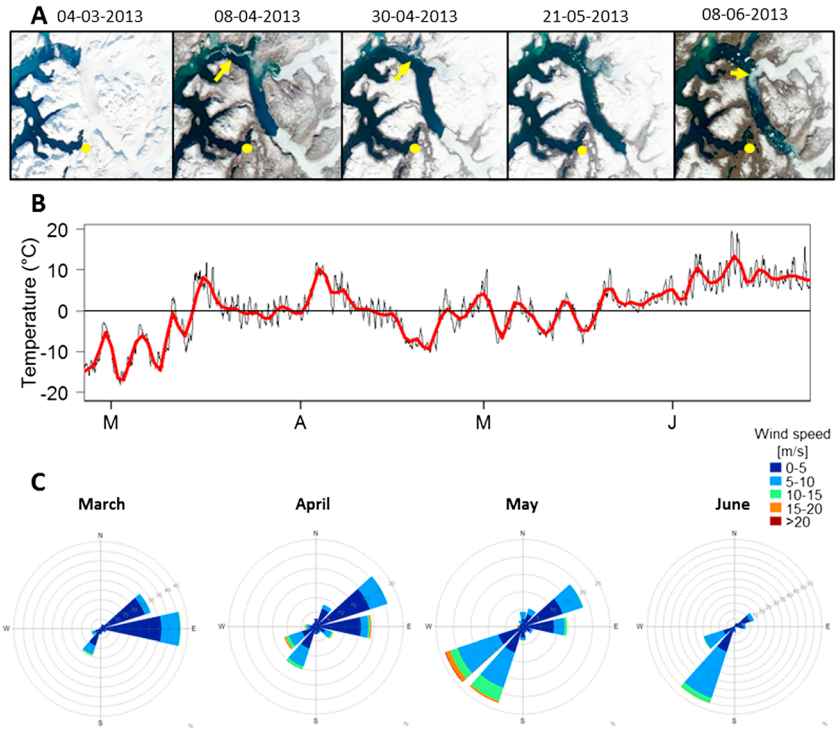

Figure 2. Ice and atmospheric conditions in Godthåbsfjord. (a) Temporal evolution of the sea ice conditions in Kangersuneq as derived from the MODIS (Moderate Resolution Imaging Spectroradiometer) instrument on board the Terra/Aqua satellites. The yellow dot indicates the Kapisillit meteorological station as reference point. The yellow arrows indicate the plume of icebergs released by Narsap Sermia glacier. (b) Air temperature (°C) as recorded from Kapisillit meteorological station. The red line represents a moving average with a filter length of 4 days. (c) Wind rose as recorded at the Kapisillit meteorological station reveals a notable change in the wind direction between March–April and May–June.

mélange in front of the KNS terminus broke up and released large amounts of glacial ice preventing further sampling in Kangersuneq (Figure 2a).

2.2. Hydrographic and Water Chemistry Data

Monthly water column sampling was conducted from March to June 2013 at three fixed stations (GF10, GF13, and GF17) in Kangersuneq (Figure 1). This temporal data set was further complemented with a spatial survey obtained during a hydrographic cruise aboard R/V *Sanna* from 7 to 15 May 2013, conducted as part of the Marine Basis Nuuk monitoring program by the Greenland Institute of Natural Resources. During this survey, water column sampling was carried out at 25 stations along a length section in Godthåbsfjord (Figure 1), from the KNS glacier terminus (near station GF18) to the continental slope at Fyllas Banke (station FB3.5). During all sampling campaigns, salinity and temperature depth profiles were recorded by CTD (Seabird SBE19+) a Seabird SBE19+, equipped with additional sensors for fluorescence (Seapoint Chlorophyll Fluorometer), oxygen (SBE 43, Seabird), and photosynthetic active radiation (Li-Cor 190SA quantum Q, Li-Cor). Partial pressure of carbon dioxide (pCO_2) was measured in situ using the HydroC™ Carbon Dioxide Sensor (Contros, Germany) at six water depths (1, 5, 10, 20, 30, and 40 m). At every depth the HydroC sensor was equilibrated for 2–5 min until a stable reading was obtained. The relative standard deviation (RSD) of the pCO_2 measurement has been estimated to be 1% [*Fietzek et al.*, 2014]. Additionally, discrete water samples were collected using a 5 L Niskin water sampler at 1, 5, 10, 20, 30, and 40 m. Water was collected from the Niskin bottle using Tygon tubing for the determination of oxygen concentrations using Winkler titration, which were used to calibrate the CTD oxygen optode. Water samples for chlorophyll *a* (Chl *a*) analysis were filtered (500 mL) through 25 mm GF/F filters (Whatman, nominal pore size of 0.7 μm). Filters were placed in 10 mL 96% ethanol for 18 to 24 h, and chlorophyll fluorescence in the filtrate was analyzed using a fluorometer (TD-700, Turner Designs) before and after addition of 200 μL of HCl solution (1 *M*). Chlorophyll *a* concentrations were used to calibrate the CTD fluorescence values. Chlorophyll *a* readings

were converted to Chl *a*-based carbon (Chl-C) using a carbon to Chl *a* ratio by weight of 40 g:g [*Lorenzen*, 1968] for comparison with collected zooplankton biomass during the May research cruise. Subsamples (10 mL) for nutrients (phosphate, silicate, and nitrate) were filtered through 0.45 μm filters (Q-Max GPF syringe filters) and frozen until further analysis. Nitrate and phosphate were measured using standard colorimetric methods on a Seal QuAAtro auto analyzer. Dissolved silicate (DSi) concentrations were analyzed on a Thermo iCAP6300 Duo-ICP.

Satellite images (Moderate Resolution Imaging Spectroradiometer (MODIS) Terra/Aqua and Landsat 8 courtesy of the U.S. Geological Survey) were analyzed to monitor the sea ice extent over the sampling period. Air temperature, wind speed and direction, and solar irradiance data were obtained from the meteorological stations in Kapisillit (Asiaq, Greenland Survey). All processing of data was done in the open-source programming language R [*R Core Team*, 2013]. Density profiles were used to calculate the stratification parameter ϕ ($J\,m^{-2}$) in the upper water layer (0–60 m), which represents the amount of energy required to fully mix the water column through vertical mixing [*Simpson*, 1981]. Euphotic depth was calculated as 1% of surface irradiance, and the mixed layer depth was defined as the depth where gradient in density is maximal. Interpolation of the data was done, and resulting contour plots were produced using the R extension package Akima [*Akima et al.*, 2006].

3. Results

3.1. Ice Conditions and Weather Conditions in the Inner Fjord

During winter, the inner part of Godthåbsfjord, Kangersuneq, is usually covered with sea ice. Although the sea ice extent varies from year to year, the ice cover typically extends to station GF13. Satellite images confirm the presence of a sea ice cover in Kangersuneq in March 2013 (Figure 2a). However, higher air temperatures prevailed from mid-March to early April 2013 (Figure 2b), and this led to an early breakup of a fraction of the sea ice in 2013, so that large parts of Kangersuneq were ice free by early April (Figure 2a). The breakup of the ice mélange in front of the Narsap Sermia glacier terminus in early April resulted in a limited release of glacial ice into the fjord (Figure 2a, 8 April). From mid-April to mid-May, air temperature decreased, and only small changes of the ice conditions in the fjord were observed (Figures 2a and 2b). During winter (January to April), the dominant wind direction in inner fjord was from northeast to east, i.e., out-fjord. Ice not being landfast was consequently blown out of the fjord, as evident from satellite images (Figure 2a) as well as visual observations during sampling.

In mid-May, the air temperature gradually increased in Kangersuneq, whereas wind speed became more variable and gradually changed direction, with southwesterly winds prevailing by the end of May, i.e., winds were mainly directed into the fjord and toward the glaciers (Figure 2c). As illustrated by the satellite images (Figure 2a, 8 June), glacial ice released from the Narsap Sermia glacier was now transported farther into the fjord, opposite to the outward transport observed earlier in spring. The presence of a stable ice mélange in the innermost part of the fjord still prevented export of calved icebergs from the KNS glacier. However, increasing air temperatures eventually led to the breakup of this ice mélange around 10 June.

3.2. Temporal and Spatial Variability of the Spring Bloom

After the breakup of sea ice in Kangersuneq in early April 2013, the inner fjord became accessible and monthly sampling campaigns were initiated at stations GF10, GF13, and GF17 (Figure 1). These surveys revealed substantial spatial gradients in hydrographic and biogeochemical parameters in the inner part of the fjord (Figures 3 and 4). In April, water temperatures at all three stations increased with depth. At stations GF13 and GF17, temperature was ~0°C at the surface and increased to 2°C at 60 m depth, while at the GF10 station farther out-fjord, the surface water was slightly warmer (~1.5°C) but had the same temperature at depth (Figure 3). Salinities varied around ~33.2 at 60 m depth at all stations, while the surface water showed a small decrease in salinity toward the glaciers, ranging from 32.5 at GF10 to 32.0 at GF17 (Figure 3). The lower salinity in the surface water likely results from freshwater runoff due to snow melt in spring. Density gradients and stratification were comparable at all three stations (Figure 3 and Table 1). Despite the similarity in physical conditions, a strong biogeochemical gradient existed between GF17 and GF13, which are only separated by ~ 30 km (Figures 3 and 4). At stations GF10 and GF13, a spring bloom occurred as indicated by elevated chlorophyll *a* concentrations (subsurface maximum of 10 $\mu g\,L^{-1}$ at GF10 and surface maximum of 15 $\mu g\,L^{-1}$ at GF13). In contrast, at station GF17, which is located less than 25 km from the KNS summer terminus, no sign

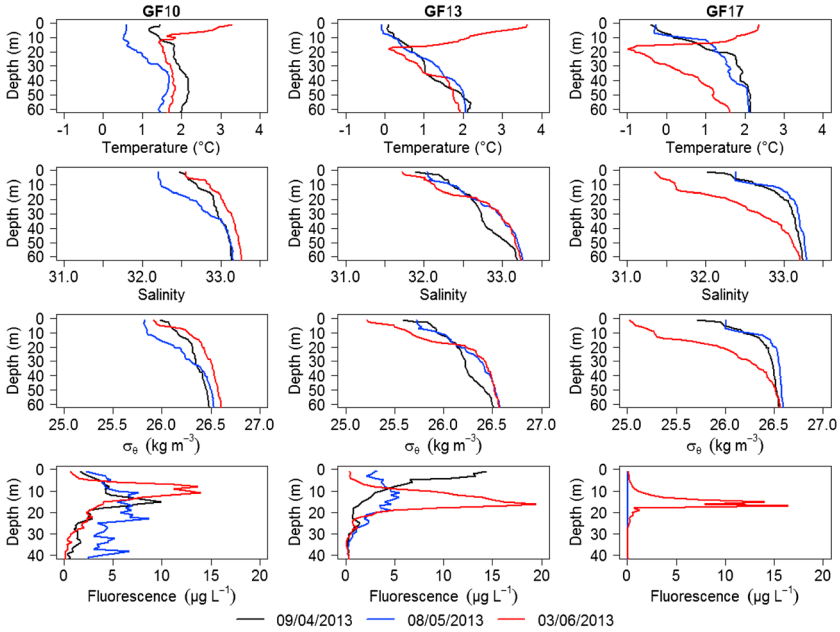

Figure 3. Temporal evolution of temperature (°C), salinity, potential density anomaly (σ_θ, kg m^{-3}), and fluorescence (calibrated versus chlorophyll *a* in µg L^{-1}) at stations GF10, GF13, and GF17 over 3 months (sampling dates are 9 April, 8 May, and 3 June 2013).

of a spring bloom was apparent as chlorophyll *a* concentrations were very low (<0.1 µg L^{-1}, observed in the CTD fluorescence and independently verified by discrete water samples). This large difference in biological activity between GF17 and the other two out-fjord stations was also reflected in the chemical parameters (Figure 4). The phytoplankton bloom at station GF10 and GF13 was confirmed by low nitrate and DSi concentrations in the upper water column, reduced pCO_2 values in the surface layer, and clear signs of oxygen production (a surface and subsurface O_2 oversaturation at GF13 and GF10, respectively). The O_2 profiles were similar in shape as the Chl *a* profiles, thus confirming primary production. In contrast, at station GF17, no sign

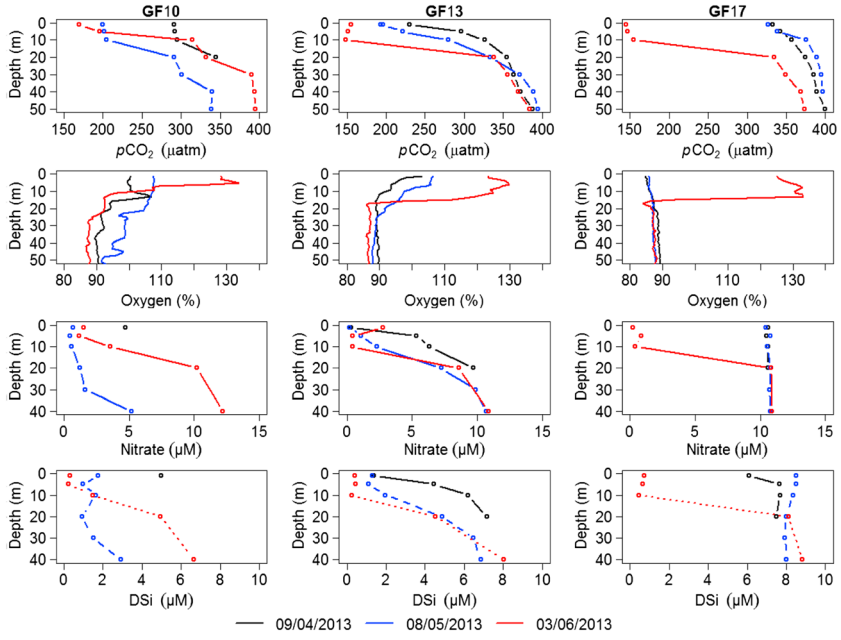

Figure 4. Temporal evolution of partial pressure of CO_2 (µatm), oxygen (% of air saturation), nitrate, and dissolved silica (DSi) (µM) at stations GF10, GF13, and GF17 over 3 months (sampling dates are 9 April, 8 May, and 3 June 2013).

Table 1. Data on Mixed Layer Depth (m), Euphotic Depth (m), Stratification Index (J m^{-2}), and Integrated Chlorophyll *a* (mg m^{-2}) at Stations GF10, GF13 and GF17 Over 3 Months (Sampling Dates Are 9 April, 8 May, and 3 June 2013)

	Station	Mixed Layer Depth (m)	Euphotic Depth (m)	Stratification Index (J m^{-2})	Integrated Chlorophyll *a* (mg m^{-2})
9 April 2013	GF10	14	14	35	120
	GF13	6	22	48	112
	GF17	7	31	40	2
8 May 2013	GF10	17	16	53	185
	GF13	8	23	61	102
	GF17	10	37	40	2
3 June 2013	GF10	6	22	41	142
	GF13	4	17	76	155
	GF17	15	26	97	62

of nutrient consumption was observed in the upper water column, while the oxygen remained undersaturated throughout the upper water column (O_2 concentrations ~300 μM, i.e., 85% of air saturation). The absence of primary production in the inner fjord station GF17 could not be attributed to light limitation, because the euphotic depth (depth where 1% light remained) was substantially deeper at GF17 (~31 m) than at GF10 (~14 m) where a subsurface Chl *a* maximum was present (Table 1).

One month later, at the beginning of May, physical conditions at all stations were still comparable to those observed in April (Figure 3). Continued primary production at station GF13 gave rise to a further reduction in nutrient levels in the surface layer, and a subsurface Chl *a* maximum was now also observed at station GF10. At the inner fjord station GF17, still no sign of primary production was observed, despite that the station was already ice free for more than a month. Chl *a* values remained low, nutrient concentrations and pCO_2 were relatively high, and oxygen was below saturation in the upper water column (Figure 4).

At the end of May, important changes in the physical settings occurred at all three stations (Figures 3 and 5). The temperature of the upper 15 m increased, and a subsurface temperature minimum developed between 10 and 20 m. This subsurface minimum was most pronounced at station GF17 closest to the KNS glacier terminus (minimum temperature of −1°C at 18 m depth). At station GF17, the water layer between 15 and 60 m showed a clear cooling compared to previous months, linked to cold water input from the KNS terminus (Figures 3 and 5). Salinity profiles at stations GF10 and GF13 remained unchanged, but at GF17, a freshening of the upper 60 m of the water column occurred, linked to the melting of ice mélange (sea ice and glacial ice)

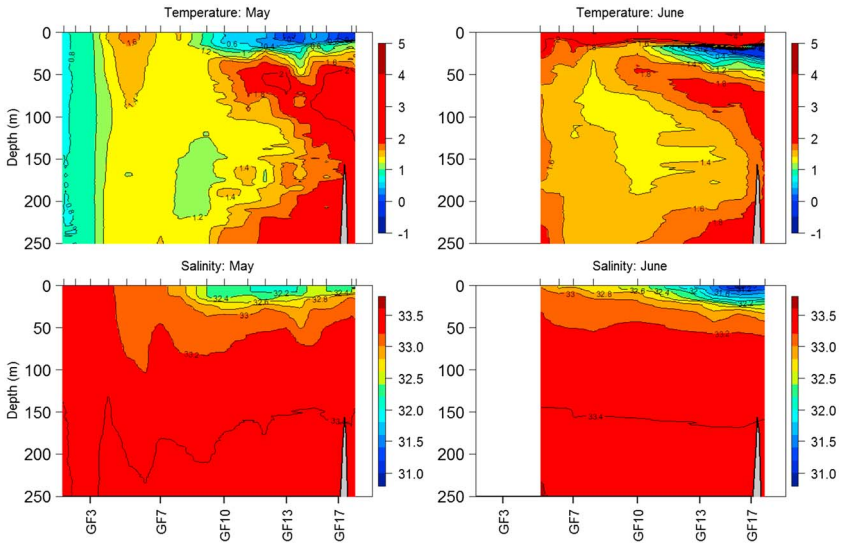

Figure 5. Length section of (top row) temperature and (bottom row) salinity for transects in Godthåbsfjord during early May (10 May) and June (4 June) from glacier (right) to fjord entrance (left).

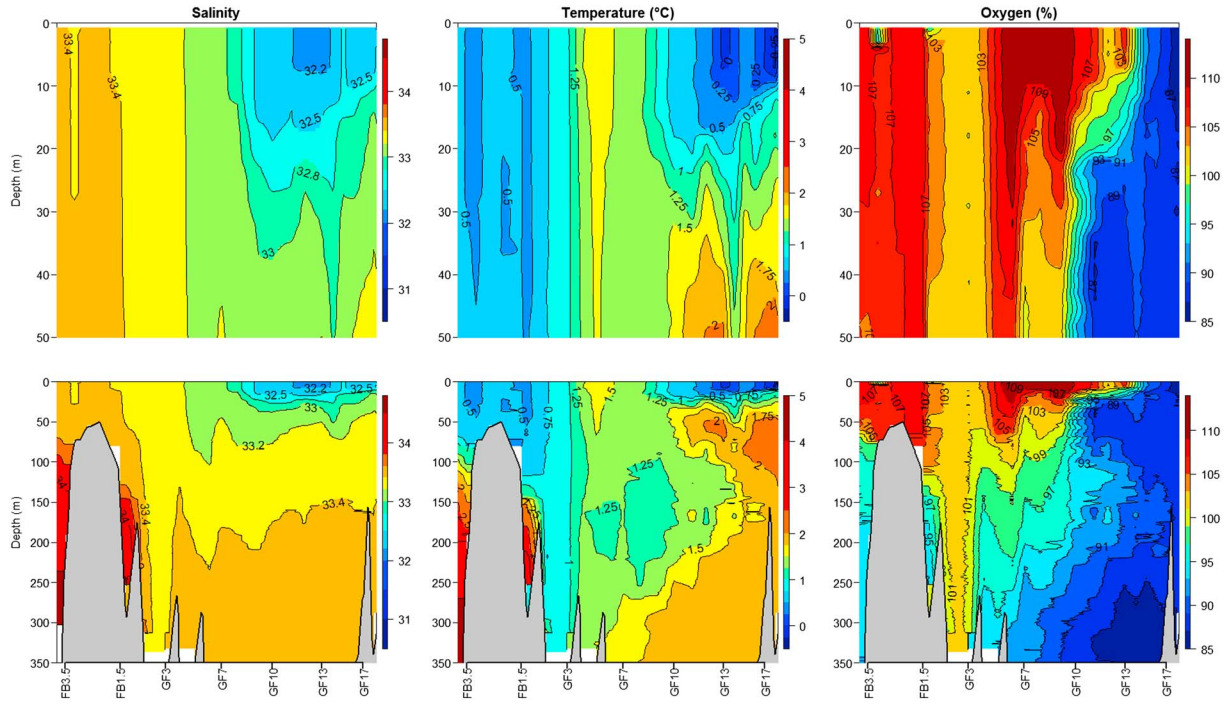

Figure 6. Length section of salinity (left), temperature (°C, middle), oxygen (% air saturation, right) in Godthåbsfjord during the May 2013 cruise from Fyllas banke shelf region (left) to the proximity of KNS glacier terminus (right). The top panel shows a close-up on the upper 50 meter.

and due to fresh water runoff. For the first time, high Chl *a* values (~15 μg L^{-1}) were observed at the inner station GF17, which were concentrated in a narrow subsurface maximum around 15 m. Concurrently, an oversaturation of oxygen (130%), a strong reduction in pCO_2 (~150 μatm), and strong nutrient (nitrate and DSi) depletion suggested strong primary production at GF17 (Figure 4). Together, these data indicate that the spring bloom had finally started at GF17, 2 months later than at the two out-fjord stations. At these stations GF10 and GF13, primary production continued, generating subsurface Chl *a* maxima (up to 20 μg L^{-1} in GF13), low surface pCO_2, high O_2, and low nitrate in the surface water layer (Figure 4).

3.3. Biogeochemical Gradients in the Fjord System During the Spring Bloom

In addition to the monthly sampling at the three fjord stations, a hydrographic survey was carried out in May 2013 along a transect from the continental slope to the inner fjord. This survey revealed substantial spatial variability (Figure 6). In the central and inner part of the fjord (GF5 to GF18), warm (1.75–2°C) and saline (~33.4) water was found at depth characterized by low oxygen concentrations (80–85% air saturation; Figure 6). Temperature and oxygen transects revealed upwelling of this warmer and oxygen-depleted water mass in the inner part of the fjord (GF15 to GF18; Figure 6). Salinities (~32) in the upper water column were only slightly lower in the inner part of the fjord, indicating limited ice melt and/or limited freshwater runoff. Toward the mouth of the fjord (GF4 to GF10), salinity and temperature of the surface layer gradually increased. The oxygen levels in the upper water column showed also an out-fjord increase, from undersaturation in the inner part of the fjord (85%) to oversaturation (110%) close to the mouth (Figure 6). Close to the entrance of the fjord (GF1 to GF4), tidal mixing in the outer sill region annihilated stratification and homogenized the entire water column, thus generating uniform temperature and salinity profiles with depth (Figure 6). At the continental slope (Fyllas Banke station FB3.5), a warm (>2°C) and saline (~34.0) water mass was present deeper than 150 m, overlain by a pycnocline between 75 and 150 m of water depth, which marked the transition to colder (~0.5°C) and slightly fresher (~33.4) surface water.

In the innermost part of Godthåbsfjord, close to the glaciers (GF17), high nutrient concentrations were observed in the upper water column (Figure 7). Combined with favorable deep light penetration, such high nutrient conditions would normally lead to the development of a phytoplankton bloom. However, the expected buildup of phytoplankton biomass and the associated consumption of nutrients were only

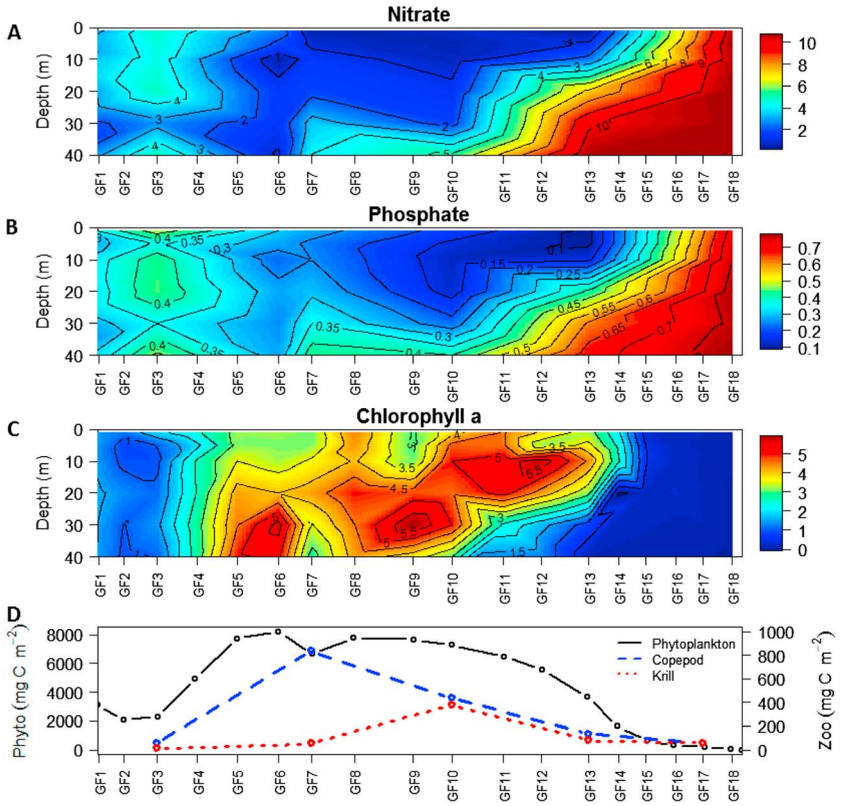

Figure 7. Length section of (a) nitrate (μM), (b) phosphate (μM), (c) chlorophyll (μg L^{-1}), and (d) integrated phytoplankton and zooplankton biomass (mg C m^{-2}) in Godthåbsfjord obtained during May 2013 cruise from mouth of the fjord (left) to KNS glacier terminus (right). Zooplankton biomass (mg C m^{-2}; Figure 7d) is redrawn from *Teglhus et al.* [2014].

observed out-fjord near station GF13, where high Chl *a* concentrations were present in the upper 10 m. Farther out-fjord in the central part of the fjord (GF10 to GF5), nutrients became gradually depleted in the surface layer, and as a result, the bloom was displaced to deeper water depths (20–40 m), giving rise to sub-surface Chl *a* peaks (concentrations ~ 5–6 μg L^{-1}). Strong tidal mixing in the outer sill region (GF1 to GF5) induced a small increase in nutrient concentrations, but Chl *a* concentrations remained low in the outer sill region, presumably due to strong downward mixing of cells below the photic zone (Figure 7). Starting from the inner fjord (station GF19), the total phytoplankton biomass (integrated over the upper 40 m, Figure 7d) showed a gradual buildup toward a maximum of 7–8 g C m^{-2} in the central part of the fjord, followed by a decrease toward the mouth of the fjord. The depth-integrated zooplankton biomass recorded during the same spatial survey (data already reported in *Teglhus et al.* [2014]; reproduced in Figure 7) exhibited a similar spatial pattern, with a peak in krill biomass around GF10 (0.38 g C m^{-2}) and maximum in copepod biomass around GF7 (0.84 g C m^{-2}) .

4. Discussion

Typically, the spring bloom accounts for a major part (50–60%) of the total annual primary production in high-latitude fjord systems [*Sakshaug*, 2004; *Juul-Pedersen et al.*, 2015; *Meire et al.*, 2015], and hence, it is important to understand the environmental factors that drive the timing and dynamics of these spring bloom events. We investigated the spring bloom development in 2013 in Godthåbsfjord, a subarctic fjord adjacent to the Greenland Ice Sheet. Sea ice cover in Godthåbsfjord only plays a limited role in the spring bloom dynamics, as the sea ice remains typically confined to the innermost part of the fjord, close to the tidewater outlet glaciers. In 2013, the sea ice cover broke up early, allowing us to study the biogeochemistry throughout spring to within 20 km of the edge of the marine terminating glaciers. This sampling campaign revealed substantial spatial gradients in the fjord where the buildup of biomass was delayed by almost 2 months in

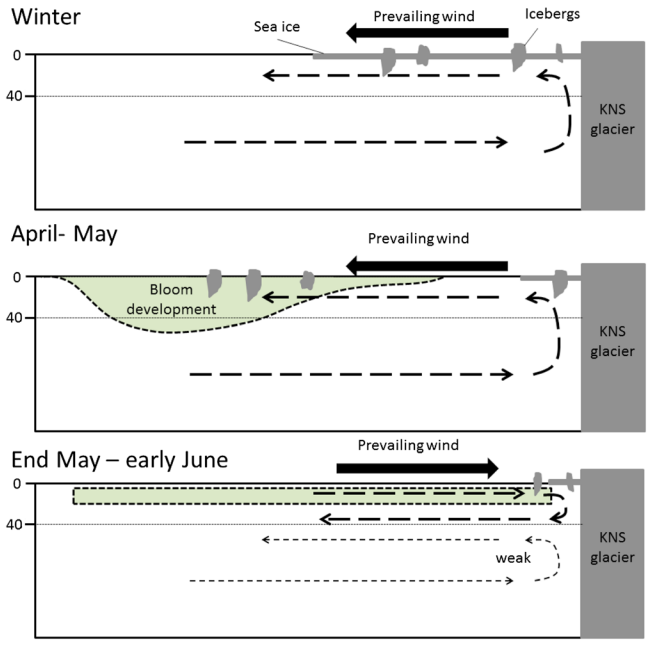

Figure 8. Conceptual model of the hydrodynamic circulation in winter, early spring (April–May), and late spring (end of May–June) in the fjord and its effect on the spring bloom dynamics. Coastal inflows and out-fjord winds are acting from winter to May and result in an out-fjord surface water transport. This causes a gradual out-fjord development of the spring bloom. From May, the coastal inflows weaken, and prevailing wind direction becomes in-fjord. This changes the hydrodynamic circulation and leads to a transport of the surface water toward the inner part of the fjord (KNS glacier terminus). The 40 m isobath is indicated in each panel. The green area delineates the location of the spring bloom.

the innermost part of the fjord. These findings suggest that the intensity and location of the spring bloom in Godthåbsfjord is controlled by an interplay of three physical factors: (1) the presence of sea ice, (2) the upwelling of nutrient-rich water, and (3) the wind forcing. First, we will discuss the impact of these physical drivers (sea ice, upwelling, and winds) on the water circulation in the fjord during the winter and spring. Subsequently, we will discuss the impact of the resulting water circulation pattern on the biogeochemistry of the fjord.

4.1. Circulation During Spring in Godthåbsfjord

The surface water circulation in Godthåbsfjord in spring is determined by the interaction between three different physical forcings: density-driven coastal inflows, fjord wind, and freshwater runoff. During winter and early spring, inflows of coastal water are observed in Godthåbsfjord, driven by density differences (mainly determined by salinity) between the shelf and the fjord (Figure 6). These inflows occur sporadically from October to April/June, and their occurrence is linked to variations in the coastal current system and the West Greenland Current [*Mortensen et al*., 2011, 2014]. As a result of the inflow of denser coastal water, the mean density in the fjord increases during winter and early spring, as described previously by *Mortensen et al*. [2011, 2014]. The coastal inflow thus causes a gradual replacement of the low-saline water that accumulated during the summer melt of the previous year. This basin water renewal also induces upwelling in the inner parts of fjord, which is supported in our observations by the upward sloping of isohalines in the inner part of the fjord in spring, as well as by the temperature and oxygen data (Figures 3 and 6). As a result of upwelling in the inner part, the water in the surface layer is pushed outward toward the fjord entrance.

The innermost part of Godthåbsfjord is normally covered with sea ice during winter, which was also the case during winter and early spring of 2013. The presence of sea ice shelters the surface waters from the wind stress and thus reduces circulation in the upper water layer (Figures 2 and 8). However, sea ice broke up early in 2013 (late March; Figure 2), and from this moment onward, fjord winds were able to act on the surface circulation. During winter, the combination of a cold Greenland Ice Sheet with (relatively) warm coastal water drives an out-fjord wind regime in many of Greenland's fjords [*Bromwich et al*., 1996]. This pattern is also apparent in Godthåbsfjord, where we observed an out-fjord wind, which was steered along the curved fjord axis due to the steep orography of the fjord (Figure 2). This strong out-fjord wind regime likely enhances the outflow of the surface water in spring and intensifies the ongoing density-driven upwelling of deeper water in the inner fjord system. These out-fjord winds also affect the iceberg transport within the fjord. Until mid-March 2013, the presence of an ice mélange kept the icebergs trapped at the glacier termini. The breakup of the ice mélange in front of Narsap Sermia typically marks the start of iceberg calving season. As seen on satellite images (Figure 2a), the calved icebergs from Narsap Sermia were exported quickly out of the fjord during April–May by the dominant out-fjord winds (Figures 8a and 8b).

In mid-May 2013, the dominant wind direction changed from out-fjord to in-fjord (Figure 2c). This change was caused by more intense heating in the inner part of the fjord, and this in-fjord wind regime is characteristic for late spring and summer in Godthåbsfjord [*Mortensen et al*., 2011]. At the end of spring, density-driven inflows of shelf water also weakens, a reoccurring pattern observed by acoustic Doppler current profiler measurements earlier [*Mortensen et al*., 2014]. Downward sloping isohalines toward the inner part of the fjord suggest downwelling at the head of the fjord (Figure 5). We hypothesize that the change in the dominant wind direction and weakening of the coastal inflows (Figure 2c) reversed the circulation in the surface near layer of the inner fjord (Figure 8). Contrary to the previous months, icebergs were no longer transported out-fjord, but as revealed by the satellite images, icebergs were actually transported into the fjord (Figure 2a). As a consequence of this new circulation mode, warm surface water was transported from the central parts of the fjord toward the KNS terminus (Figure 5). Below the warmer surface layer, a cold water mass (at 10 to 40 m depth) indicates the necessary return flow, where the cold water temperatures are associated with the melting of the ice mélange near the glacier terminus.

During May 2013, the glacial melt season had not started yet, as discharge of glacial rivers was still low [*van As et al*., 2014]. But aside direct solar heating (and higher air temperatures, Figure 2b), wind-driven advection of warm surface water is another potential heat source for melt of the ice mélange near the glacier termini (Figures 3 and 5). Summarizing our observations, we hence propose a circulation pattern in late spring, which is characterized by an in-fjord wind, a weak upwelling in the inner fjord, and a counterflow just below the stratified surface water (as depicted in Figure 8c).

4.2. Development of the Spring Bloom in Godthåbsfjord

Our data revealed a clear pattern in the timing and spatial extent of the spring bloom in Godthåbsfjord, which can be linked to the changes in water circulation regime as described above. Light limitation and increased vertical mixing generally prevents the development of a spring bloom in winter where Chl *a* concentrations are low ($<0.1\ \mu g\ L^{-1}$) [*Juul-Pedersen et al*., 2015; *Meire et al*., 2015]. Increased solar radiation, combined with increased stratification due to melting of the calved icebergs in the fjord and runoff due to snow melt in spring, subsequently creates favorable conditions for a phytoplankton bloom (Figure 3). The spring bloom started to develop in Godthåbsfjord in April 2013, though not at the innermost stations close to the KNS glacier terminus (Figure 4). Despite comparable stratification and light levels (Table 1), a strong spatial gradient was observed between the in-fjord station GF17 and the out-fjord stations GF10 and GF13. From early April to May, a continuous phytoplankton bloom was observed at stations GF10 and GF13, while over the same period, Chl *a* concentrations remained low at GF17 (located ~50 km in-fjord). Our hydrographic surveys indicated that upwelling occurred in the inner fjord section (close to GF17), which supplied nutrient-rich water to the surface waters during the spring months (Figures 4 and 6). This provided a continuous supply of nutrients needed to sustain the spring bloom in the fjord system (Figure 8b), which was both extensive in space (covering the section from the fjord mouth to GF13) as prolonged in time (April–June). The observed patterns in primary production are further supported by undersaturation of oxygen and relatively high pCO_2 levels close to station GF17, while oxygen oversaturation and low pCO_2 levels were observed at the out-fjord stations (GF10 and GF13) (Figure 4) [*Meire et al*., 2015].

As stratification and light climate conditions are comparable between stations (Table 1), a difference in grazing pressure by zooplankton could be an explanation for the absence of a spring bloom in April–May near the glacier front. Data on zooplankton biomass and grazing experiments however show that the grazing impact is low (maximum 15% of phytoplankton community, [*Teglhus*, 2014]), suggesting that physical drivers must play a dominant role. So why did the spring bloom not develop close to glacier, i.e., at station GF17? The deep nutrient-rich water that upwells in the inner fjord section is low in phytoplankton spores as indicated by the low chlorophyll values and cell counts at GF18 (observed during May cruise on R/V *Sanna*). Therefore, we hypothesize that the absence of a phytoplankton bloom at the inner most station GF17 is due to a spatially displaced buildup of phytoplankton biomass. The upwelling of deep waters near the glacier termini induces an out-fjord circulation of surface water. While the surface water flows out-fjord, the phytoplankton population gradually builds up from a low seeding population, and so the actual bloom only manifests itself at GF13 and further toward the mouth of the fjord (GF10 and beyond). Based on a doubling time of 0.4 to 0.6 per day for diatoms at 0°C [*Eppley*, 1972; *Gilstad and Sakshaug*, 1990] and with observed chlorophyll *a* values of $0.1\ \mu g\ L^{-1}$ at GF17, it is possible to estimate the distance for a bloom to develop. Assuming no grazing,

it takes 10–12 days to reach Chl *a* values of 5 to 10 μg L^{-1}. With an estimated surface current in Godthåbsfjord of around 5 cm s^{-1}, this implies that it takes a distance of 42 to 66 km for the bloom to develop. This estimate is in general accordance with the distance (~50 km) between the KNS terminus and station GF13, where the bloom became first noticeable. Although the phytoplankton growth rates and the advective time scale were not measured directly, our first-order calculation supports the hypothesis that phytoplankton growth was ongoing during the out-fjord transit of upwelled water but that sizeable biomass accumulation only manifested itself farther downstream.

As noted above, the sea ice broke up early in Godthåbsfjord in 2013. The sea ice extent will affect the area and location where the "delayed" spring bloom can develop. In years where the inner fjord is more extensively covered by sea ice, we hypothesize that upwelling will take place under the sea ice and that this upwelling will also drive an out-fjord flow of the surface water. Hence, the sea ice edge will determine the location where light can first penetrate and the buildup of phytoplankton biomass can start. Accordingly, in years with a larger sea ice cover, we speculate that the same type of bloom dynamics goes on but that the location of the phytoplankton bloom will be shifted to more out-fjord stations (i.e., at a roughly constant distance from the sea ice edge). Previous surveys, undertaken in Godthåbsfjord during spring, support the delayed spring bloom model that is proposed here. A study by *Arendt et al*. [2010] shows a similar upwelling in the inner fjord region of Godthåbsfjord with a subsequent delayed development of a phytoplankton bloom further out-fjord. Observations from the mouth of Godthåbsfjord support the hypothesis that a large fraction of the biomass is exported toward the mouth of the fjord and dispersed throughout the entire water column due to strong tidal mixing within the sill region [*Juul-Pedersen et al*., 2015].

High phytoplankton biomass was only observed at GF17 at the end of May, indicating that the spring bloom did eventually initiate at this station, albeit with a delay of almost 2 months. In a period of 20 days, nutrients were strongly depleted in the upper 10 m at station GF17, while a strong oversaturation in O_2 and an undersaturation in CO_2 developed (Figure 4). These observations match with the observed circulation changes in the upper layer (section 4.1 and Figure 8c), where surface water was driven toward the inner fjord.

4.3. Conclusions and Outlook

Local upwelling driven by density inflows, in combination with fjord winds, resulted in an outward transport of surface water in Godthåbsfjord during spring. This circulation pattern plays an important role in the spring bloom dynamics of the fjord system (Figure 8). The upwelling of nutrient-rich water in the inner part of the fjord results in a gradual buildup of a high phytoplankton biomass in the fjord (Figures 4 and 7). Biological uptake causes a gradual depletion of nutrients in the upper water layer, which then leads to a concomitant decrease in plankton biomass as one move toward the sill region (Figure 7). The prolonged and intense phytoplankton bloom in the fjord forms an important food source for higher trophic levels and sustains a high zooplankton biomass [*Arendt et al*., 2010; *Teglhus et al*., 2014] (Figure 7). Therefore, changes in fjord circulation patterns linked to changes in dominant winds and fjord-ocean exchange in addition to changes in sea ice cover can have large implications on spring bloom dynamics in high-latitude fjord systems.

Acknowledgments
This study was supported by the Research Foundation Flanders (FWO aspirant grant to L.M.) and received financial support from IIKNN Greenland. S.R. was funded by the Canada Excellence Research Chair program. J.M. was financially supported by DEFROST under Nordic Centers of Excellence (NCoE) program. F.J.R.M. received funding from the European Research Council under the European Union's Seventh Framework Programme (FP7/2007-2013) via ERC grant agreement (306933). We thank Asiaq Greenland Survey for supplying the meteo data. This study was conducted in collaboration with the marine monitoring program MarineBasis-Nuuk, part of the Greenland Ecosystem Monitoring (GEM), and forms a contribution to the Arctic Science Partnership (ASP) and the ArcticNet Networks of Centers of Excellence programs.

References

Akima, H., A. Gebhardt, T. Petzoldt, and M. Maechler (2006), Akima: Interpolation of irregularly spaced data, *R Packag. version 0.5-1*. [Available at http://CRAN.R-project. org/package=akima.]

Arendt, K., T. Nielsen, S. Rysgaard, and K. Tönnesson (2010), Differences in plankton community structure along the Godthåbsfjord, from the Greenland Ice Sheet to offshore waters, *Mar. Ecol. Prog. Ser.*, *401*, 49–62, doi:10.3354/meps08368.

Arrigo, K. R., G. van Dijken, and S. Pabi (2008), Impact of a shrinking Arctic ice cover on marine primary production, *Geophys. Res. Lett.*, *35*, L19603, doi:10.1029/2008GL035028.

Bromwich, D. H., Y. Du, and K. M. Hines (1996), Wintertime surface winds over the Greenland Ice Sheet, *Mon. Weather Rev.*, *124*(9), 1941–1947, doi:10.1175/1520-0493(1996)124<1941:WSWOTG>2.0.CO;2.

Degerlund, M., and H. C. Eilertsen (2010), Main species characteristics of phytoplankton spring blooms in NE Atlantic and Arctic Waters (68–80°N), *Estuaries Coasts*, *33*(2), 242–269, doi:10.1007/s12237-009-9167-7.

Eilertsen, H. C., and S. Frantzen (2007), Phytoplankton from two sub-Arctic fjords in northern Norway 2002–2004: I. Seasonal variations in chlorophyll *a* and bloom dynamics, *Mar. Biol. Res.*, *3*(5), 319–332, doi:10.1080/17451000701632877.

Eilertsen, H. C., J. P. Taasen, and J. M. Wesiawski (1989), Phytoplankton studies in the fjords of west Spitzbergen: Physical environment and production in spring and summer, *J. Plankton Res.*, *11*(6), 1245–1260, doi:10.1093/plankt/11.6.1245.

Eppley, R. W. (1972), Temperature and phytoplankton growth in the sea, *Fish. Bull.*, *70*, 1063–1085.

Fietzek, P., B. Fiedler, T. Steinhoff, and A. Körtzinger (2014), In situ quality assessment of a novel underwater pCO_2 sensor based on membrane equilibration and NDIR spectrometry, *J. Atmos. Oceanic Technol.*, *31*(Dic), 181–196, doi:10.1175/JTECH-D-13-00083.1.

Gilstad, M., and E. Sakshaug (1990), Growth rates of ten diatom species from the Barents Sea at different irradiances and day lengths, *Mar. Ecol. Prog. Ser.*, *64*, 169–173, doi:10.3354/meps064169.

Hegseth, E. N., and V. Tverberg (2013), Effect of Atlantic water inflow on timing of the phytoplankton spring bloom in a high Arctic fjord (Kongsfjorden, Svalbard), *J. Mar. Syst.*, *113-114*(2013), 94–105, doi:10.1016/j.jmarsys.2013.01.003.

Hodal, H., S. Falk-Petersen, H. Hop, S. Kristiansen, and M. Reigstad (2012), Spring bloom dynamics in Kongsfjorden, Svalbard: Nutrients, phytoplankton, protozoans and primary production, *Polar Biol.*, *35*, 191–203, doi:10.1007/s00300-011-1053-7.

Juul-Pedersen, T., K. Arendt, J. Mortensen, M. Blicher, D. Søgaard, and S. Rysgaard (2015), Seasonal and interannual phytoplankton production in a sub-arctic tidewater outlet glacier fjord, west Greenland, *Mar. Ecol. Prog. Ser.*, *524*, 27–38, doi:10.3354/meps11174.

Lorenzen, C. J. (1968), Carbon/chlorophyll relationships in an upwelling area, *Limnol. Oceanogr.*, *13*(1), 202–204, doi:10.4319/lo.1968.13.1.0202.

Meire, L., D. H. Søgaard, J. Mortensen, F. J. R. Meysman, K. Soetaert, K. E. Arendt, T. Juul-Pedersen, M. E. Blicher, and S. Rysgaard (2015), Glacial meltwater and primary production are drivers of strong CO_2 uptake in fjord and coastal waters adjacent to the Greenland Ice Sheet, *Biogeosciences*, *12*(8), 2347–2363, doi:10.5194/bg-12-2347-2015.

Mortensen, J., K. Lennert, J. Bendtsen, and S. Rysgaard (2011), Heat sources for glacial melt in a sub-Arctic fjord (Godthåbsfjord) in contact with the Greenland Ice Sheet, *J. Geophys. Res.*, *116*, C01013, doi:10.1029/2010JC006528.

Mortensen, J., J. Bendtsen, R. J. Motyka, K. Lennert, M. Truffer, M. Fahnestock, and S. Rysgaard (2013), On the seasonal freshwater stratification in the proximity of fast-flowing tidewater outlet glaciers in a sub-Arctic sill fjord, *J. Geophys. Res. Ocean.*, *118*, 1382–1395, doi:10.1002/jgrc.20134.

Mortensen, J., J. Bendtsen, K. Lennert, and S. Rysgaard (2014), Seasonal variability of the circulation system in a west Greenland tidewater outlet glacier fjord, Godthåbsfjord (64°N), *J. Geophys. Res. Earth Surf.*, *119*, 2591–2603, doi:10.1002/2014JF003267.

R Core Team (2013), R development core team, *R A Lang. Environ. Stat. Comput.*

Rysgaard, S., and R. N. Glud (2007), Carbon cycling and climate change: Predictions for a high Arctic marine ecosystem (Young Sound, NE Greenland), *BioScience*, *58*, 206–214.

Rysgaard, S., T. G. Nielsen, and B. W. Hansen (1999), Seasonal variation in nutrients, pelagic primary production and grazing in a high-Arctic coastal marine ecosystem, Young Sound, Northeast Greenland, *Mar. Ecol. Prog. Ser.*, *179*(Digby 1953), 13–25, doi:10.3354/meps179013.

Sakshaug, E. (2004), Primary and secondary production in the Arctic Seas. in *The Organic Carbon Cycle in the Arctic Ocean*, edited by R. Stein, and R. W. Macdonald, pp. 57–81, Springer, Berlin.

Simpson, J. H. (1981), The shelf-sea fronts: Implications of their existence and behaviour, *Philos. Trans. R. Soc. A Math. Phys. Eng. Sci.*, *302*(1472), 531–543, doi:10.1098/rsta.1981.0181.

Storr-Paulsen, M., K. Wieland, H. Hovgård, and H. J. Rätz (2004), Stock structure of Atlantic cod (Gadus morhua) in West Greenland waters: Implications of transport and migration, *ICES J. Mar. Sci.*, *61*(6), 972–982, doi:10.1016/j.icesjms.2004.07.021.

Sverdrup, H. (1953), On conditions for the vernal blooming of phytoplankton, *J. Du Cons.*, doi:10.4319/lom.2007.5.269.

Syvitski, J. P. M., D. C. Burrell, and J. M. Skei (1987), *Fjords*, Springer, New York.

Teglhus, F. W., M. D. Agersted, K. E. Arendt, and T. G. Nielsen (2014), Gut evacuation rate and grazing impact of the krill *Thysanoessa raschii* and *T. inermis*, *Mar. Biol.*, doi:10.1007/s00227-014-2573-9.

Tett, P., and A. Wallis (1978), The general annual cycle of chlorophyll standing crop in Loch Creran, *J. Ecol.*, *66*(1), 227–239, doi:10.2307/2259190.

van As, D., et al. (2014), Increasing meltwater discharge from the Nuuk region of the Greenland ice sheet and implications for mass balance (1960–2012), *J. Glaciol.*, *60*(220), 314–322, doi:10.3189/2014JoG13J065.

Wu, Y., I. K. Peterson, C. C. L. Tang, T. Platt, S. Sathyendranath, and C. Fuentes-Yaco (2007), The impact of sea ice on the initiation of the spring bloom on the Newfoundland and Labrador Shelves, *J. Plankton Res.*, *29*(6), 509–514, doi:10.1093/plankt/fbm035.